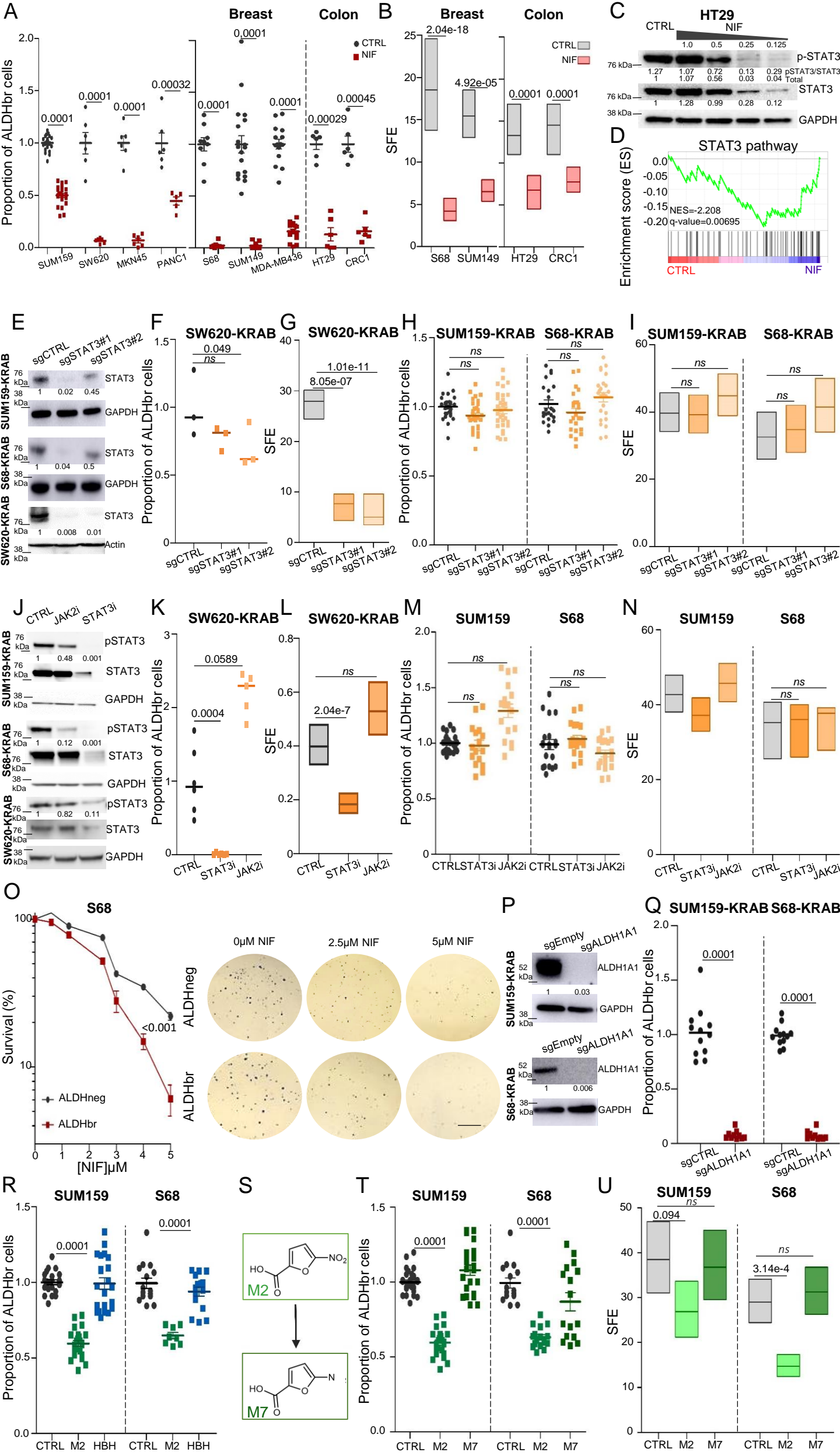
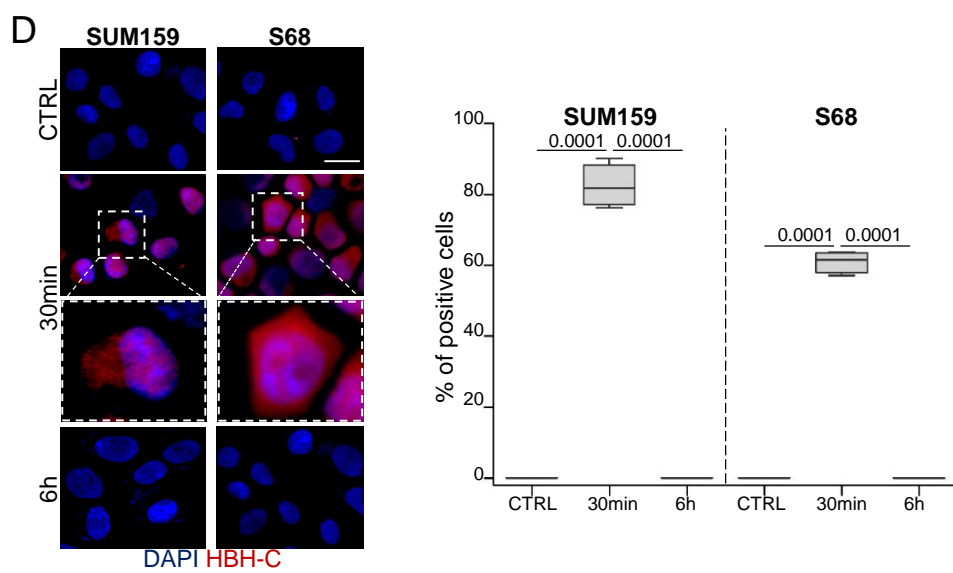
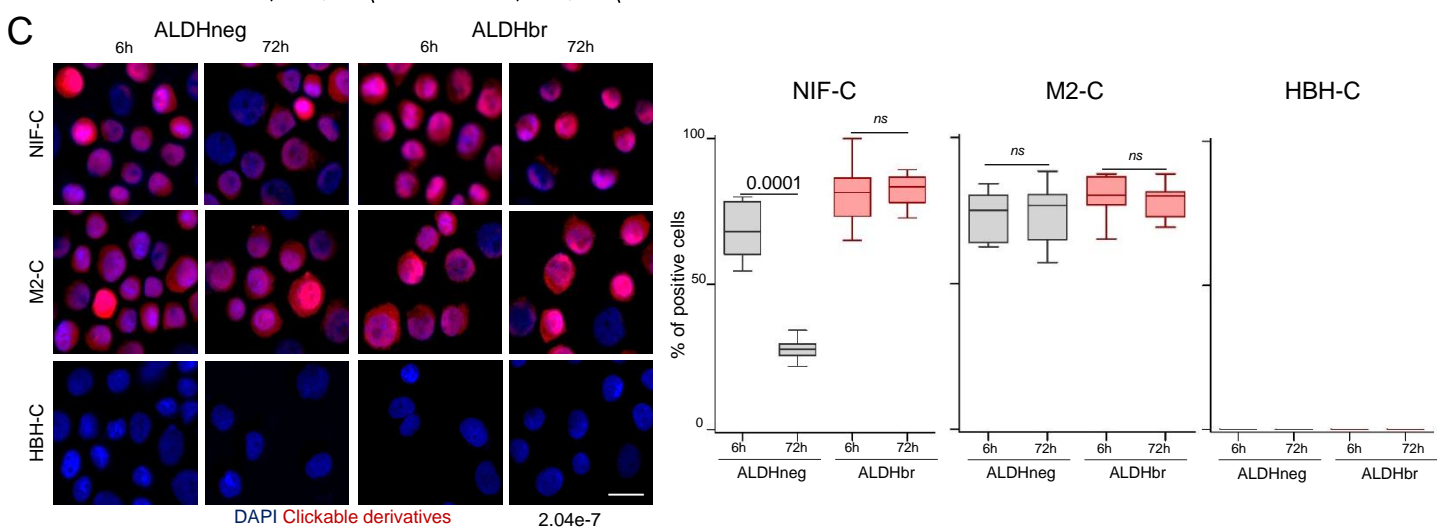
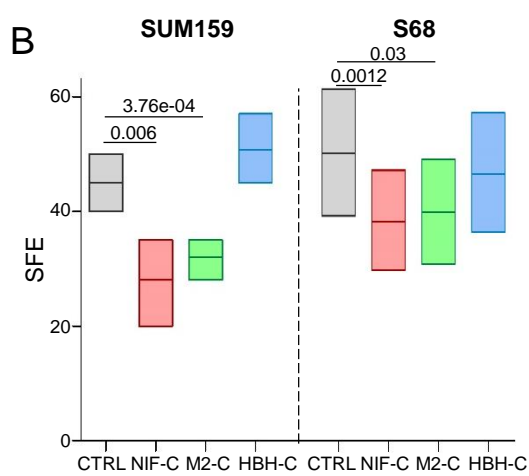
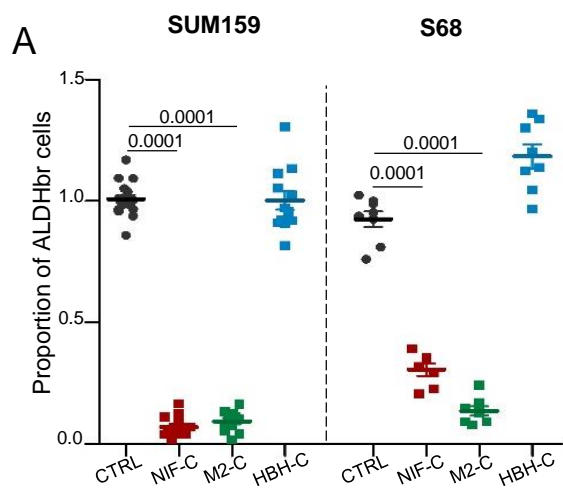


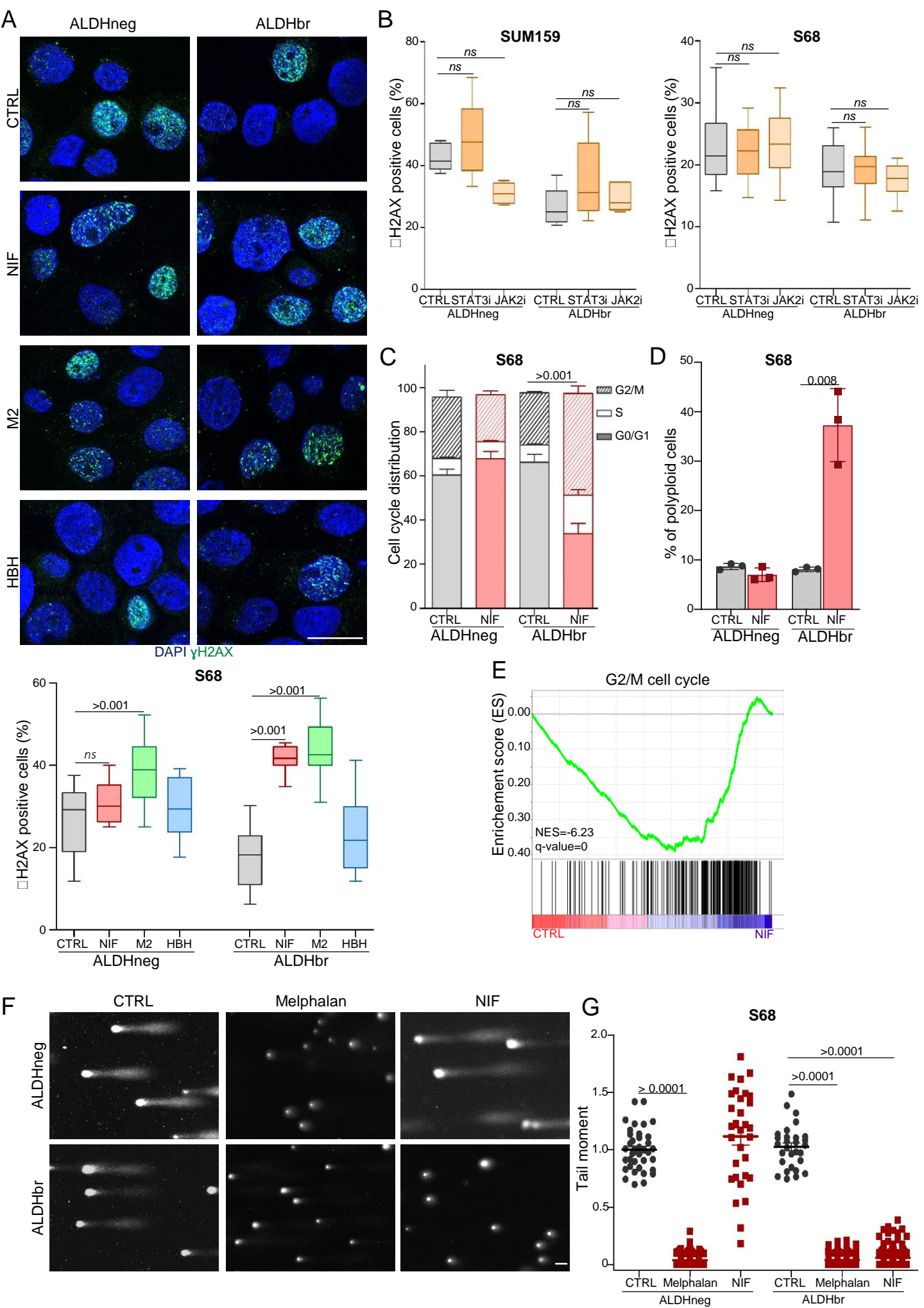
Supplementary Information of Inhibition of the STAT3/Fanconi anemia axis is synthetic lethal with PARP inhibition in breast cancer



Supplementary Figure 1. The anti-CSC compound Nifuroxazide is bioactivated by ALDH and inhibits STAT3 signalling. **A.** Proportion of ALDHbr cells following NIF treatment compared with the untreated condition (CTRL). **B.** SFE of breast and colon cell lines under treatment with NIF compared with the untreated condition (CTRL). (n=6). **C.** Western blot of STAT3 and p-STAT3 in NIF-treated HT29 colon cells compared to untreated conditions (CTRL). The mean intensities are indicated below each band for each condition from n=3 independent experiments. **D.** Pre-ranked GSEA interrogating differential expression between ALDHbr CTRL and NIF treated SUM159 and SW620 cells of genes involved in STAT3 pathway. **E.** Western blot of STAT3 SUM159-KRAB, S68-KRAB and SW620-KRAB with sgCTRL or sgSTAT3. The mean intensities are indicated below each band for each condition from n=3 independent experiments. **F,H.** Proportion of ALDHbr cells in colon (SW620-KRAB) and breast (SUM159-KRAB and S68-KRAB) cells with sgCTRL or sgSTAT3. **G,I.** SFE of colon (SW620-KRAB) and breast (SUM159-KRAB, S68-KRAB) cells with sgCTRL or sgSTAT3. **J.** Western blot of p-STAT3 and STAT3 SUM159-KRAB, S68-KRAB and SW620-KRAB following 24H of STAT3i or JAK2i treatment. The mean intensities are indicated below each band for each condition from n=3 independent experiments. **K,M.** Proportion of ALDHbr cells following STAT3i and JAK2i treatment compared with the untreated condition (CTRL). **L,N.** SFE of SW620, SUM159 and S68 under STAT3i and JAK2i treatment. **O.** S68 cells exposed to various concentrations of NIF were subjected to clonogenic survival assays and representative images (right panel). Scale bar: 1 cm. **P.** Western blot of ALDH1A1 in SUM159-KRAB and S68-KRAB with sgEmpty and sgALDH1A1 constructs. The mean intensities are indicated below each band for each condition from n=3 independent experiments. **Q.** Proportion of ALDHbr cells in SUM159-KRAB and S68-KRAB with sgEmpty or sgALDH1A1. **R,T.** Proportion of ALDHbr cells exposed to the M2, HBH or M7 treatments compared to untreated conditions (CTRL). **S.** Chemical structure of M2 and M7 metabolites. **U.** SFE of SUM159 and S68 exposed to M2 or M7 treatment compared to the untreated condition (CTRL). In (**B, G, I, L, N, U**) box represents mean \pm margin of error (95% Confidence Interval) of n=3 independent experiments. Statistical significance was calculated using one-sided Chi-squared test or t-test. In (**A, F, H, K, M, Q, R, T**) data are shown as mean \pm SEM (Standard Error of Mean) of n=3 independent experiments, according to two-way ANOVA followed by Sidak multiple range test. ns (not significant). Source data are provided as a Source Data file.



Supplementary Figure 2. NIF clickable analogs effect on CSC and in situ detection. **A.** Proportion of ALDHbr cells following click compounds treatment compared with the untreated condition (CTRL). **B.** SFE of SUM159 and S68 after click compounds treatment compared to the untreated conditions (CTRL). **C.** Detection of NIF-C, M2-C and HBH-C (red staining) in ALDHneg and ALDHbr S68 cells after 6 and 72 hours of treatment. Nuclei are counterstained with DAPI (blue staining). Scale bar: 3.5 μ m. Box plot represent the proportion of cell with positive click-labelling after different time of treatment. **D.** Detection of HBH-C (red staining) in SUM159 and S68 cells after 30minutes and 6 hours of treatment. Nuclei are counterstained with DAPI (blue staining). Third line represents an enlargement of the area delimited by dashed line. Scale bar: 3.5 μ m. Box plot represents the proportion of cell presenting a positive click- after different times of treatment. In (**A**, **C-D**) boxplots represent median and quartile and whiskers minimum to maximum. In (**B**) box represents mean \pm margin of error (95% Confidence Interval) of n=3 independent experiments. ns (not significant), p-value estimated according to one-sided Fisher test (**A**), One-sided chi-squared test (**B**) and one-way ANOVA followed by Dunn's multiple comparison test (**C-D**). Source data are provided as a Source Data file.



Supplementary Figure 3. NIF treatment effect on DNA integrity and cell cycle progression

A. Representative images of γ H2AX foci (green staining) in ALDHneg and ALDHbr S68 cells after NIF and M2 treatment compared to the untreated conditions (CTRL). Nuclei are counterstained with DAPI (blue staining). Scale bar: 15 μ m. Box plots (bottom panel) represent the proportion of γ H2AX -positive cells (median and quartiles) with whiskers (minimum to maximum), for each cell subpopulation under the indicated treatment. (n=4).

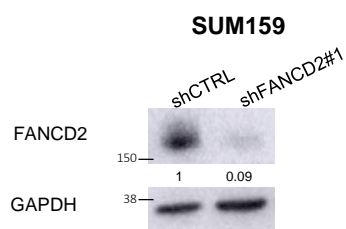
B. Box plot represents the proportion of γ H2AX -positive cells in SUM159 and S68 for each cell subpopulations (ALDHneg and ALDHbr) after 3 days of STAT3 inhibitor (STAT3i) or JAK2 inhibitor (JAK2i) treatment. Box plot show (median and quartiles) with whiskers (minimum to maximum).

C-D. Monitoring of cell cycle distribution by QIBC in ALDHneg or ALDHbr S68 cells exposed to NIF (C). Quantification of the proportion of polyploid cells (D). Data are presented as mean values +/-SD.

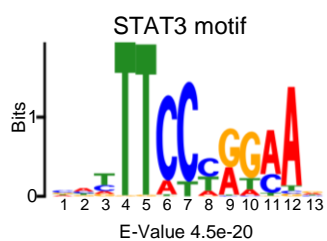
E. GSEA interrogating differential expression between ALDHbr CTRL and NIF-treated SUM159 cells of genes involved in G2/M cell cycle signalling.

F-G. Representative images of reverse comet assays conducted in ALDHbr and ALDHneg S68 cells subjected to the indicated treatments (F). Reverse comet assay quantification each dot corresponding to tail moment of one comet with the indicated drugs. Mean and SD are indicated (G). In (**A, B**) boxplots represent median and quartile and whiskers minimum to maximum. In (**C-D, G**) data are shown as mean +/- SEM of n=3 independent experiments. ns (not significant), p-value estimated according to one-way ANOVA followed by Dunn's multiple comparison test (**A, B**), or one-sided Fisher test (**C-D, G**). Source data are provided as a Source Data file.

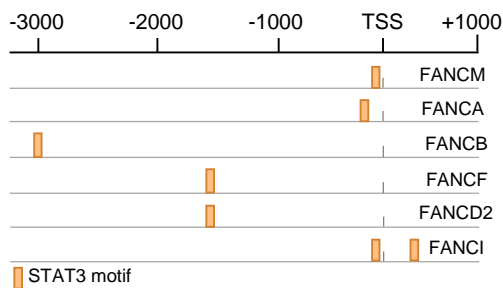
A



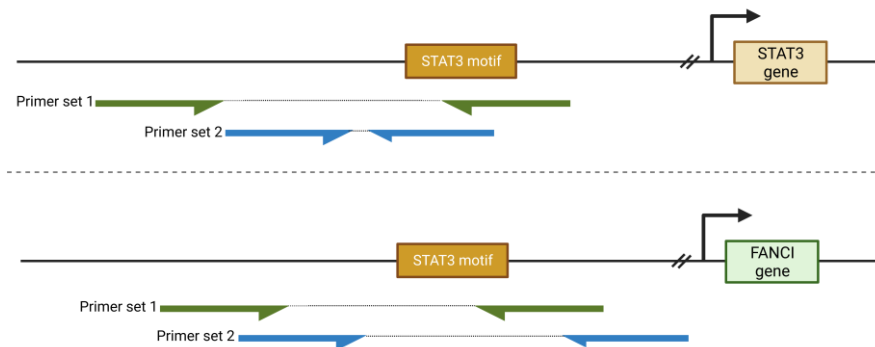
B



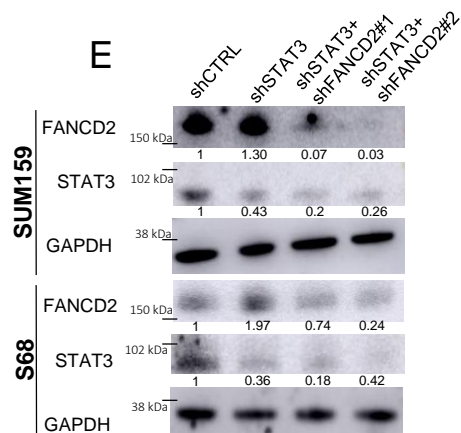
C



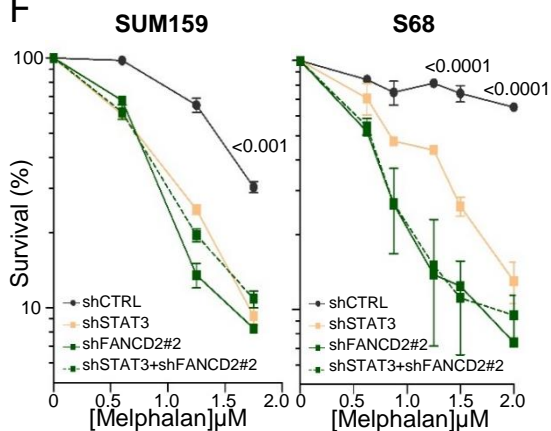
D



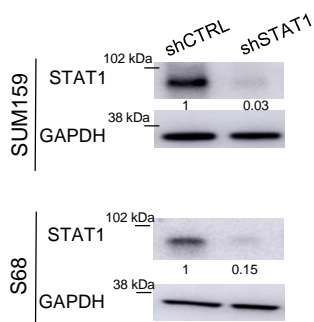
E



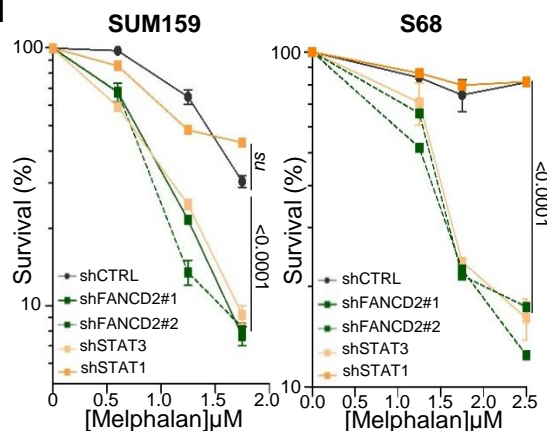
F



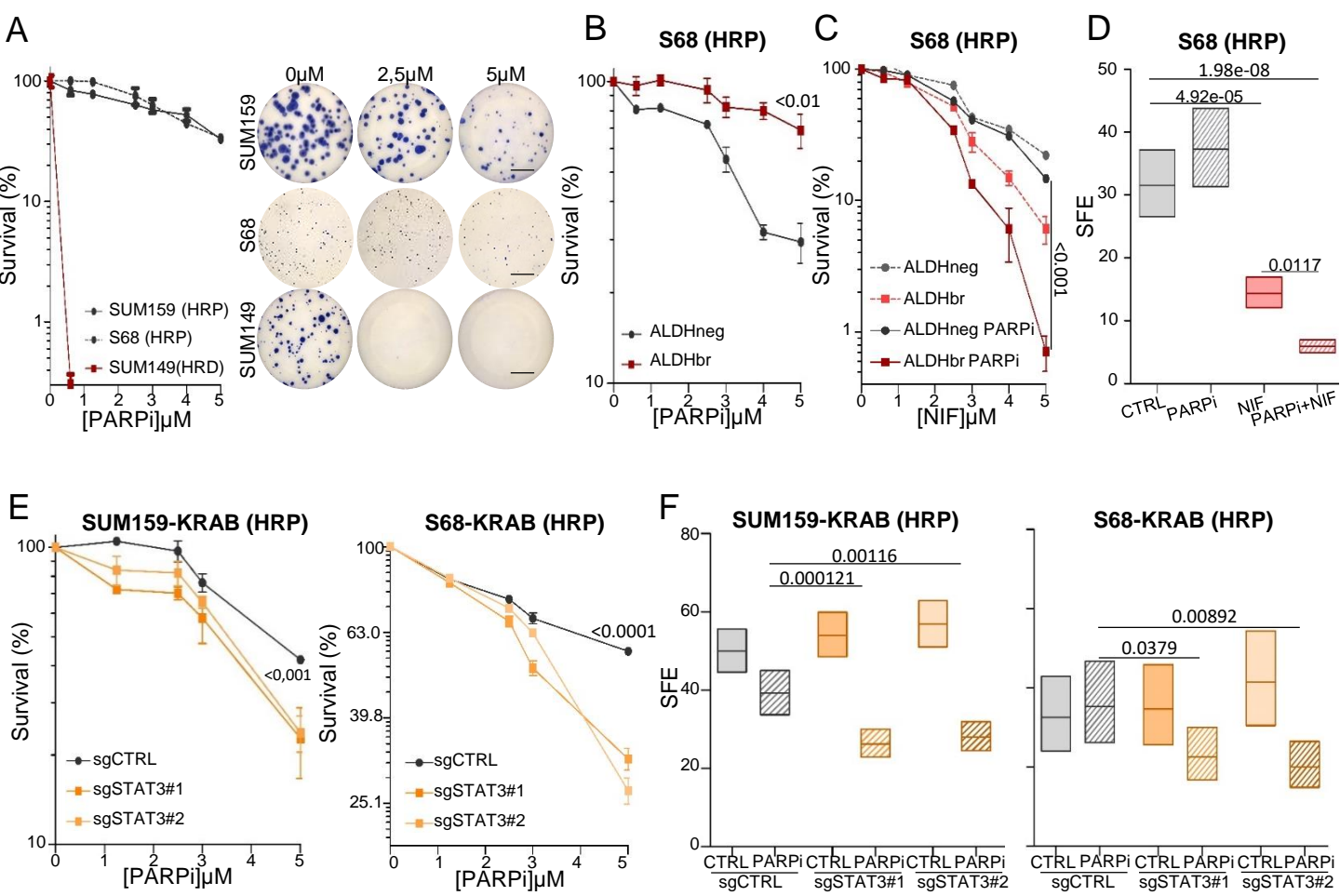
G



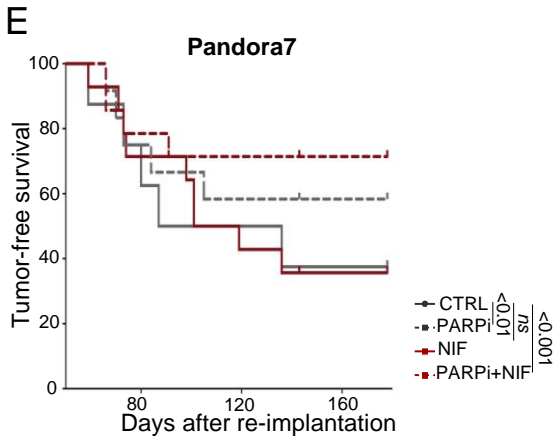
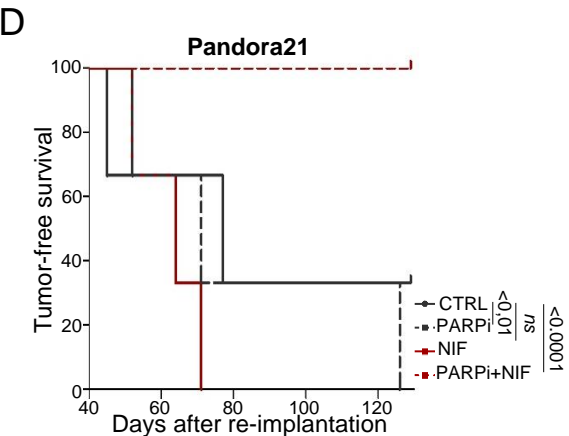
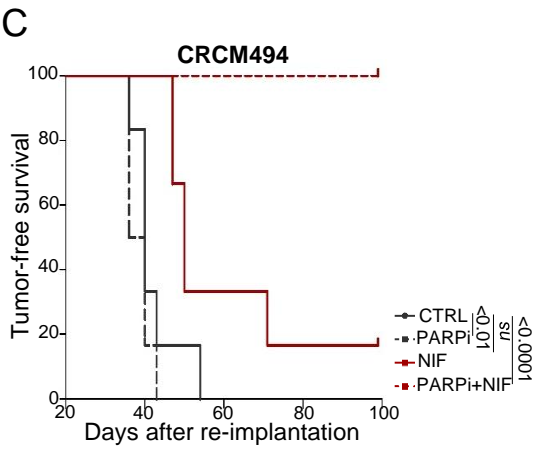
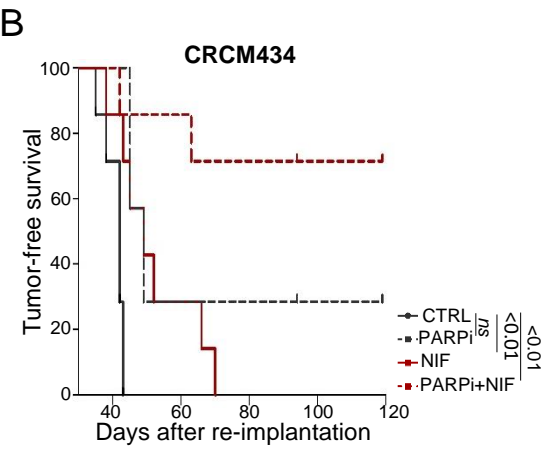
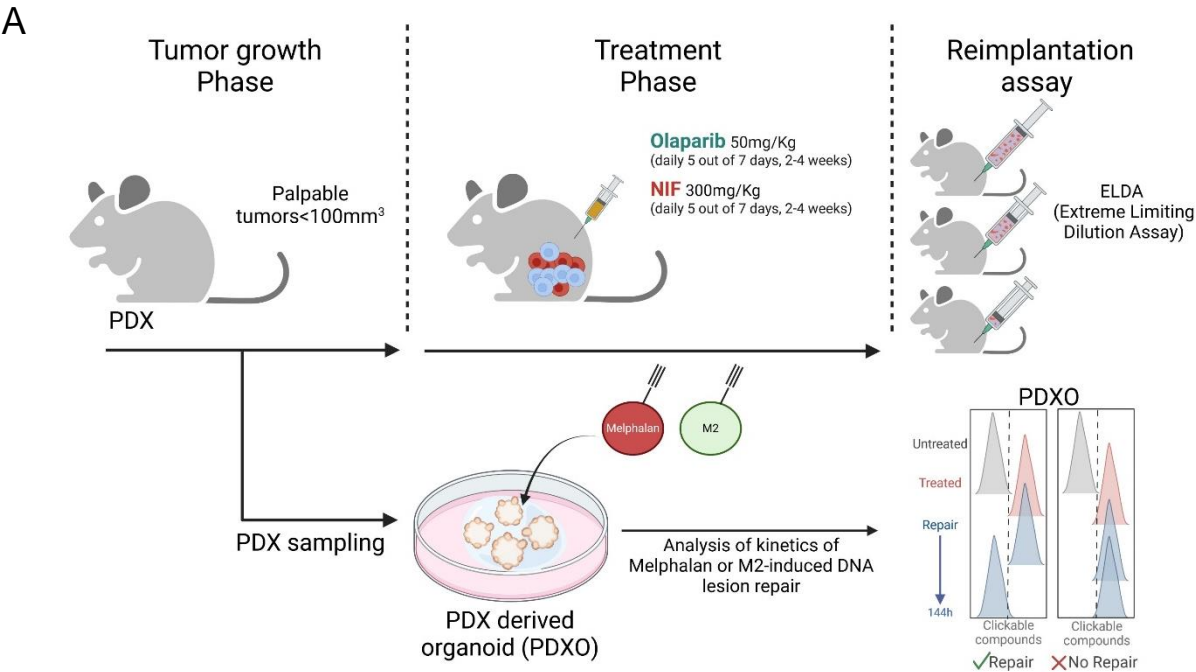
H



Supplementary Figure 4. STAT3 and Fanconi anemia pathways interaction. **A.** Western blot of FANCD2 in shCTRL and shFANCD2#1 SUM159. The mean intensities are indicated below each band for each condition from n=3 independent experiments. **B-C.** STAT3 motif enrichment in FA pathway genes promoter (B) and its location on FA pathway genes promoter (C). **D.** Location on DNA sequence of STAT3 and FANCI primer set used for CUT&RUN-qPCR analysis. **E.** Detection of FANCD2 and STAT3 protein expression in shCTRL, shFANCD2 and shSTAT3 SUM159 and S68 cell protein extracts, using western blot. The mean intensities are indicated below each band for each condition from n=3 independent experiments. **F.** SUM159 and S68 shCTRL, shFANCD2#2 and shSTAT3 cells exposed to various concentrations of melphalan were subjected to clonogenic survival assays. **G.** Detection of STAT1 protein expression in shCTRL and shSTAT1 SUM159 and S68 cell protein extracts. The mean intensities are indicated below each band for each condition from n=3 independent experiments. **H.** SUM159 and S68 shCTRL, shFANCD2, shSTAT3 shFANCD2#1 or #2 and shSTAT1 cells exposed to various concentrations of melphalan were subjected to clonogenic survival assays. In (F, H) data are shown as mean +/- SEM of n=3 independent experiments. ns (not significant), p-value estimated according to two-way ANOVA followed by sidak multiple range test. Source data are provided as a Source Data file.

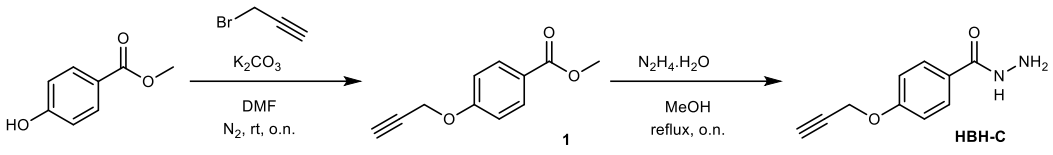


Supplementary Figure 5. Identification of synthetic lethality interaction between STAT3 and PARP inhibitions. **A.** SUM159, S68 and SUM149 cells exposed to various concentrations of PARPi were subjected to clonogenic survival assays each dot represent a mean value with SD (left panel), and representative images (right panel). Scal bar: 2.5cm for SUM159 and SUM149, 1.25cm for S68. **B-C.** S68 (HRP) ALDHneg and ALDHbr cells exposed to various concentrations of PARPi were subjected to clonogenic survival assays (**C**). S68 ALDHneg and ALDHbr cells treated with a sublethal dose of PARPi (or untreated cells) were exposed to various concentrations of NIF and subjected to clonogenic survival assays (**D**). Each dot represents a mean value with SD. **D.** SFE of S68 in NIF, PARPi on combination-treated conditions. , The box represents the confidence interval (mean and the maximum and minimum values) of n=3 independent experiments. **E.** SUM159-KRAB and S68-KRAB cells with sgCTRL or sgSTAT3 exposed to various concentrations of PARPi were subjected to clonogenic survival assays; each dot represents a mean value with SD. **F.** SFE of SUM159-KRAB and S68-KRAB cells with sgCTRL or sgSTAT3 and treated to PARPi. The box represents the confidence interval (mean and the maximum and minimum values) of n=3 independent experiments. In (**A-B, E**) data are shown as mean +/- SD of n=3 independent experiments and in (**D, F**) box represents mean \pm margin of error (95% Confidence Interval) of n=3 independent experiments. ns (not significant), p-value estimated according to and one-way ANOVA followed by Dunn's multiple comparison test (**A-B, E**) and one-sided chi-squared test (**D, F**). Source data are provided as a Source Data file.

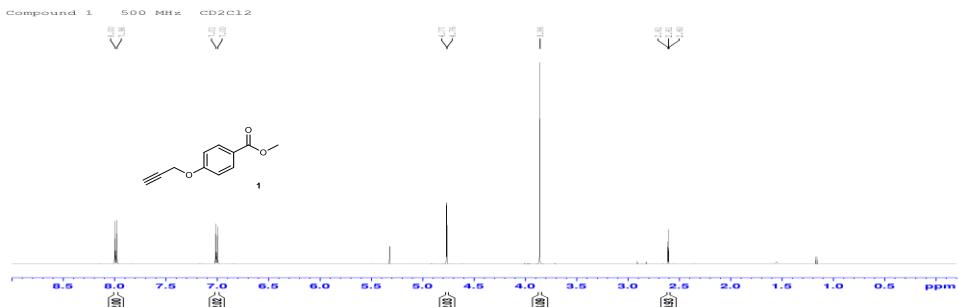


Supplementary Figure 6. Preclinal assay testing the effect of Olaparib and Nifuroxazide treatment on breast tumor relapse capacity. **A.** Schematic representation of the in vivo experimental design. Created with BioRender.com. <https://BioRender.com/b62d917>. **B-E.** Kaplan-Meier tumor-free survival curves of mice xenografted with 5-100 residual cells from treated tumors for each PDX model (n=8). ns (not significant), p-value estimated according to Log-rank (Mantel-Cox) test. Source data are provided as a Source Data file.

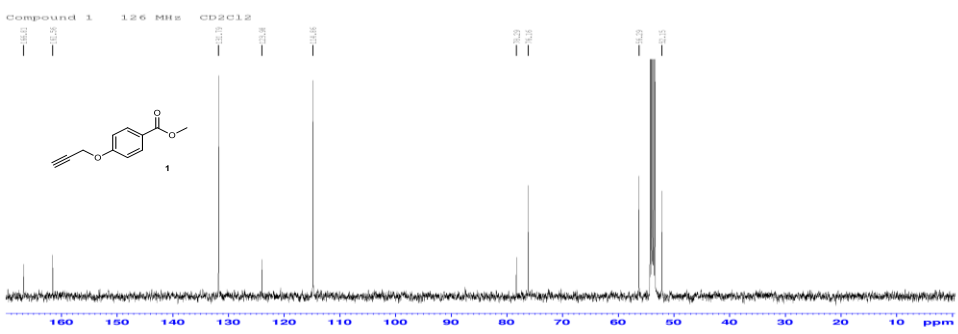
A



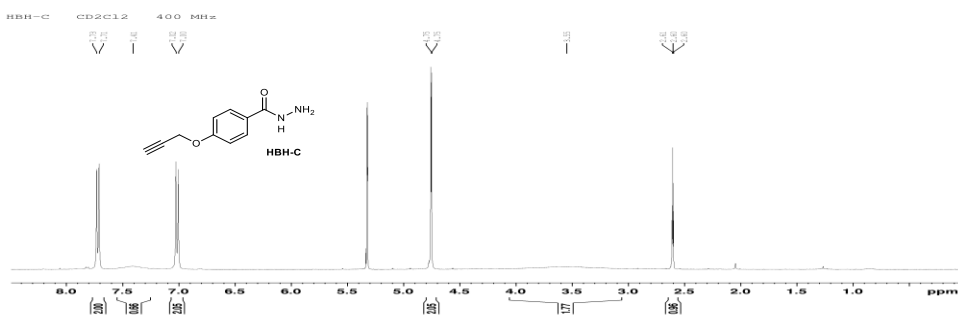
B



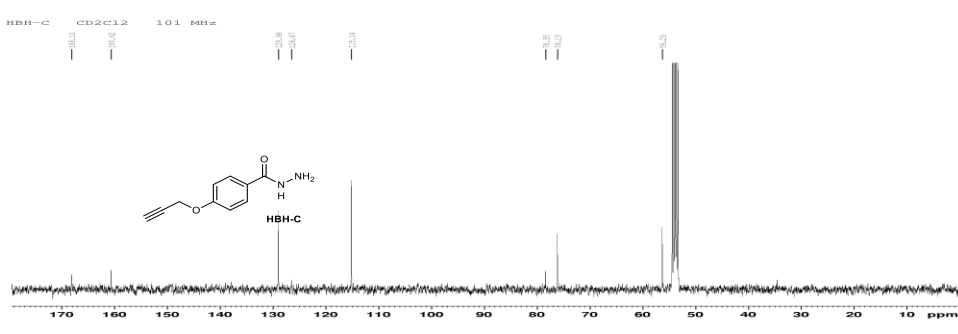
C



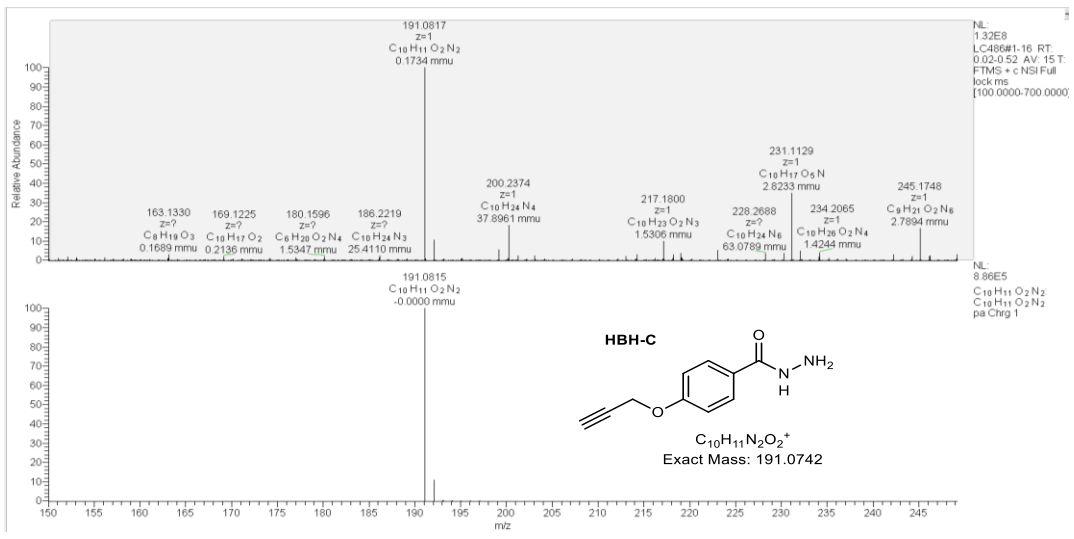
D



E



F



Supplementary Figure 7. 5-Spectroscopic and spectrometric analysis of synthesized compound 1 and HBH-C. **A.** Clickable HBH analog HBH-C procedure synthesis. **B.** ^1H NMR spectrum of compound 1 in dichloromethane- d_2 . Yield: 370 mg, 97%. Isolated as a pale brownish solid, >95% pure by NMR and a single spot by TLC; R_f : 0.63 in n-Hex/EtOAc, 80/20. ^1H NMR (500 MHz, CD_2Cl_2) δ ppm = 7.99 (d, J = 8.1 Hz, 2H), 7.00 (d, J = 8.1 Hz, 2H), 4.76 (d, J = 2.4 Hz, 2H), 3.86 (s, 3H), 2.61 (t, J = 2.4 Hz, 1H). **C.** ^{13}C NMR spectrum of compound 1 in dichloromethane- d_2 . ^{13}C NMR (126 MHz, CD_2Cl_2) δ ppm = 166.8; 161.6; 131.8 (2C); 124.0; 114.9 (2C); 78.3; 76.2; 56.3; 52.2. UPLC: R_T : 1.33 (classic system). **D.** ^1H NMR spectrum of HBH-C in dichloromethane- d_2 . Yield: 148 mg, 74%. Isolated as a white powder, >95% pure by NMR; ^1H NMR (400 MHz, CD_2Cl_2) δ ppm = 7.71 (d, J = 8.5 Hz, 2H), 7.40 (brs, 1H), 7.01 (d, J = 8.9 Hz, 2H), 4.75 (d, J = 2.5 Hz, 2H), 3.55 (brs, 2H), 2.60 (t, J = 2.5 Hz, 1H). **E.** ^{13}C NMR spectrum of HBH-C in dichloromethane- d_2 . ^{13}C NMR (101 MHz, CD_2Cl_2) δ ppm = 168.1; 160.6; 128.9 (2C); 126.5; 115.1 (2C); 78.4; 76.1; 56.3. UPLC: R_T : 1.36 (classic system). **F.** HRMS spectrum of HBH-C. HRMS (ESI $^+$) m/z $[\text{M}+\text{H}]^+$ Calcd for $\text{C}_{10}\text{H}_{11}\text{N}_2\text{O}_2^+$ 191.0742; Found 191.0817. Source data are provided as a Source Data file.

Reaction scheme showing the synthesis of NIF-C from NIF:

NIF (4-hydroxy-N-(2-nitro-5-furyl)benzamide) reacts with propargyl bromide ($\text{Br-CH}_2\text{-C}\equiv\text{CH}$) in the presence of Cs_2CO_3 in DMF at 40°C overnight (o. n.) to yield NIF-C (4-hydroxy-N-(2-nitro-5-furyl)-N-(prop-1-yn-1-yl)benzamide).

NIF-C CD3CN 500 MHz

Chemical structure of NIF-C is shown:

Oc1ccc(cc1)C(=O)N(C#C)C2=CC(=CC=C2)[N+](=O)[O-]

¹H NMR spectrum (CD₃CN, 500 MHz) of NIF-C. The spectrum shows peaks at 7.59, 7.57, 7.56, 7.55, 7.45, 6.99, 6.96, 4.90, 4.90, 2.63, 2.63, 2.62, 2.62 ppm. Integration values are 1.00, 2.08, 0.43, 1.00, 2.99, 1.98, 0.95.

NIF-C CD₃CN 126 MHz

159.90 150.80 153.22 133.83 129.17 125.76 115.27 114.50 77.43 74.59 32.45

HO NIF-C

Oc1ccc(cc1)C(=O)N(C#C)/N=C/c2cc([N+](=O)[O-])co2

ppm

Oc1ccc(cc1)C(=O)N(N=Cc2cc([N+](=O)[O-])co2)CC#C

NIF-C
 $C_{15}H_{12}N_2O_6^+$
 Exact Mass: 314.0699

NL:
 2.94E7
 LC484F2#1-16 RT:
 0.02-0.52 AV 15 T:
 FTMS + c NSI Full
 lock.ms
 [100.0000-700.0000]

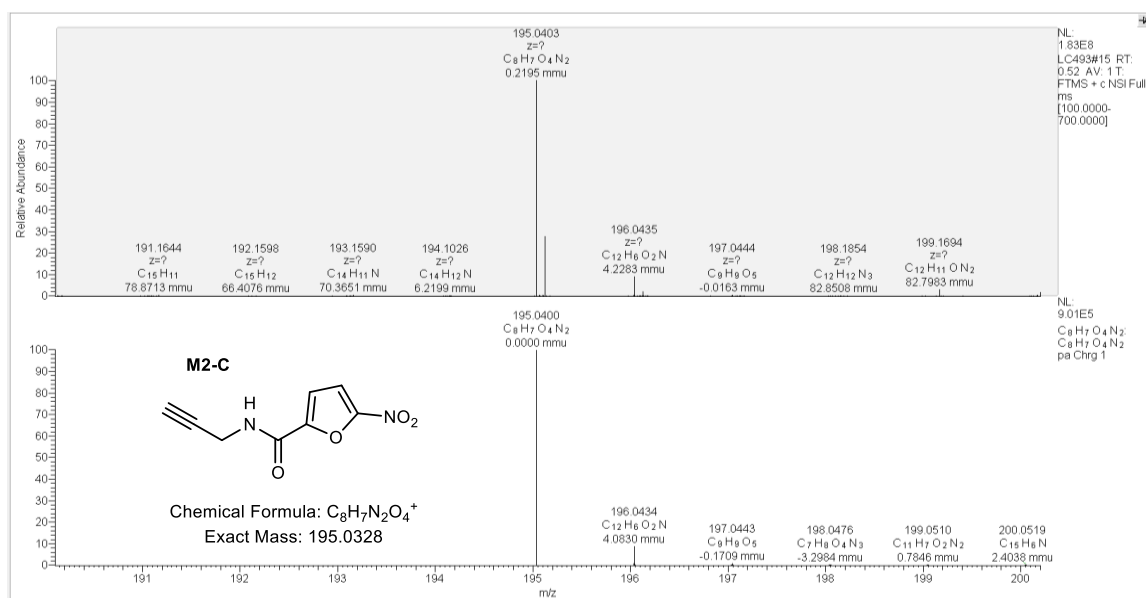
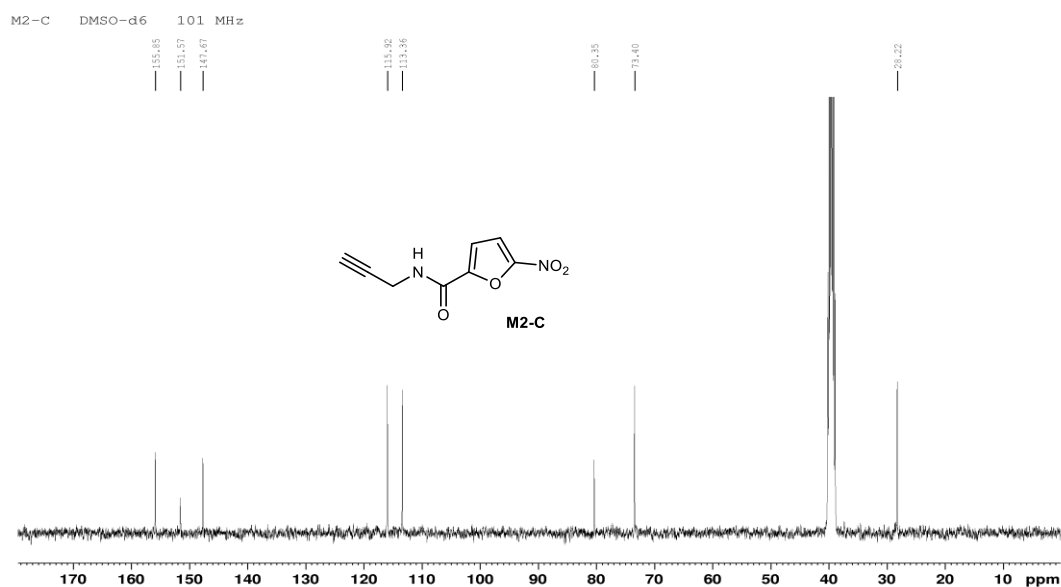
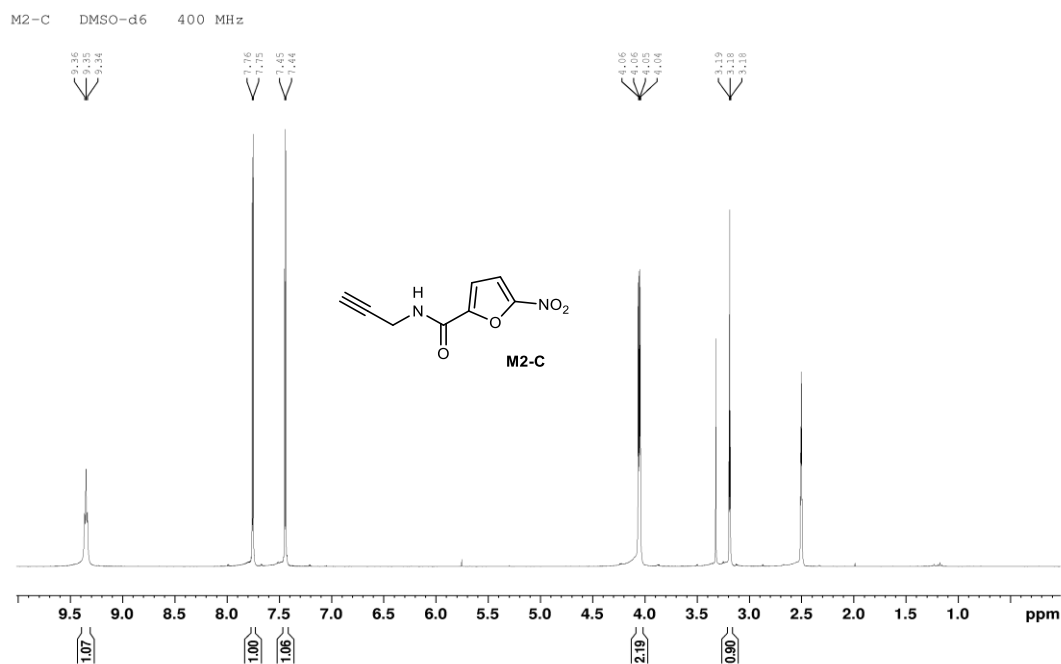
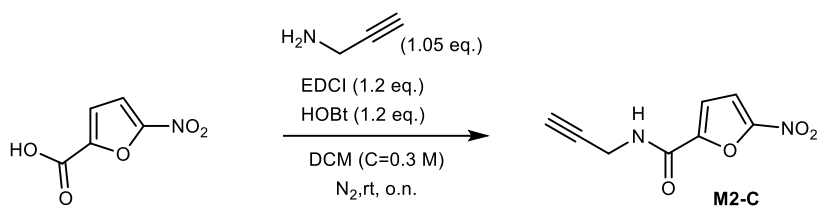
NL:
 8.30E5
 C₁₅H₁₂O₆N₂
 C₁₅H₁₂O₅N₃
 pe Chrg 1

m/z	Relative Abundance (%)	Formula	Mass Error (mmu)
306.3003	~10	z ²⁺	
306.2796	~10	z ²⁺	
310.2224	~20	z ²⁺	
310.2224	~20	C ₁₅ H ₁₂ O ₅ N ₃	124.9334
313.1434	~20	z ²⁺	
313.1434	~20	C ₁₅ H ₁₆ O ₅ N ₃	22.4662
314.0771	100	z ¹⁺	-0.0919
314.0771	100	C ₁₅ H ₁₂ O ₅ N ₃	-0.0919
314.3417	~10	z ²⁺	
315.0604	~25	z ¹⁺	
315.0604	~25	C ₁₉ H ₁₁ O ₃ N ₂	3.9838
317.2435	~10	z ²⁺	
317.2435	~10	C ₁₉ H ₁₅ O ₂ N ₃	127.6517
318.3003	~10	z ²⁺	
319.3037	~10	z ²⁺	
321.2385	~10	z ²⁺	
321.2385	~10	C ₁₈ H ₁₅ O ₃ N ₃	127.7040

m/z	Relative Abundance (%)	Formula	Mass Error (mmu)
314.0771	100	z ¹⁺	-0.0000
314.0771	100	C ₁₅ H ₁₂ O ₅ N ₃	-0.0000
315.0805	~25	z ¹⁺	
315.0805	~25	C ₁₉ H ₁₁ O ₃ N ₂	4.0830
317.0647	~10	C ₁₈ H ₁₂ O ₄	3.9122
318.0881	~10	C ₁₈ H ₁₄ O ₄	-0.5581
320.0923	~10	C ₁₉ H ₁₄ O ₄ N	0.6137
321.0957	~10	C ₁₉ H ₁₅ O ₄ N	-3.8595

Supplementary Figure 8. 5-Spectroscopic and spectrometric analysis of synthesized NIF-C.

A. Clickable NIF analog NIF-C procedure synthesis. **B.** ^1H NMR spectrum of NIF-C in dichloromethane- d_2 . Yield: 15 mg, 9.6%. Isolated as a yellow powder, >95% pure by NMR and a single spot by TLC; R_f : 0.72 in n-Hex/EtOAc, 20/80. ^1H NMR (500 MHz, CD_3CN) δ ppm = 7.89 (s, 1H), 7.70 (d, J = 8.8 Hz, 2H), 7.45 (d, J = 3.9 Hz, 1H), 6.87 (m, 3H), 4.90 (d, J = 2.7 Hz, 2H), 2.63 (t, J = 2.6 Hz, 1H). **C.** ^{13}C NMR spectrum of NIF-C in dichloromethane- d_2 . ^{13}C NMR (126 MHz, CD_3CN) δ ppm = 169.9; 160.8; 153.2 (2C) ; 133.8 (2C) ; 129.2 ; 125.8 ; 115.3 (2C) ; 114.8; 114.3 ; 77.2; 74.6; 32.5. UPLC: R_T : 2.08 (classic system). **D.** HRMS spectrum of NIF-C. HRMS (ESI $^+$) m/z $[\text{M}+\text{H}]^+$ Calcd for $\text{C}_{15}\text{H}_{12}\text{N}_3\text{O}_5^+$ 314.0699; Found 314.0771. Source data are provided as a Source Data file.



Supplementary Figure 9. 5-Spectroscopic and spectrometric analysis of synthesized M2-C. **A.** Clickable M2 analog M2-C procedure synthesis. **B.** ^1H NMR spectrum of M2-C in dichloromethane- d_2 . Yield: 331 mg, 85%. Isolated as a yellowish solid, >95% pure by NMR and a single spot by TLC; R_f : 0.6 in n-Hex/EtOAc, 50/50. ^1H NMR (400 MHz, DMSO- d_6) δ ppm = 9.34 (t, J = 5.5 Hz, 1H), 7.75 (d, J = 3.9 Hz, 1H), 7.44 (d, J = 3.9 Hz, 1H), 4.05 (dd, J = 2.6 Hz, J = 5.7 Hz, 2H), 3.18 (t, J = 2.5 Hz, 1H). **C.** ^{13}C NMR spectrum of M2-C in dichloromethane- d_2 . ^{13}C NMR (101 MHz, DMSO- d_6) δ ppm = 155.9; 151.6; 147.7 ; 115.9 ; 113.4 ; 80.4 ; 73.4 ; 28.2. UPLC: R_T : 1.59 (classic system). **D.** HRMS spectrum of M2-C. HRMS (ESI $^+$) m/z $[\text{M}+\text{H}]^+$ Calcd for $\text{C}_8\text{H}_7\text{N}_2\text{O}_4^+$ 195,0328; Found 195.0403. Source data are provided as a Source Data file.

Supplementary Table 1. Listing of treatment dose for each cell lines and corresponding compounds.

[illegible]